Indian J Phys (August 2023) 97(9):2649–2655
https://doi.org/10.1007/s12648-023-02599-x

ORIGINAL PAPER

Realization of atomically flat single terminated surface of $SrTiO_3$ (001), (110), and (111) substrate by chemical etching

A Kumari, A Gupta, S Goyal, R Kaur and S Chakraverty*

Quantum Materials and Devices Unit, Institute of Nano Science and Technology, Sector-81, Sahibzada Ajit Singh Nagar, Punjab 140306, India

Received: 15 June 2022 / Accepted: 08 January 2023 / Published online: 27 January 2023

Abstract: The research on perovskite oxide thin films, interfaces, and super-lattices demands the need for the atomically flat surface of the substrate to realize high-quality epitaxial thin films. In this paper, we report the pH-dependent Buffered NH_4F-HF (BHF) etching and concentration-dependent ACID etching of the $SrTiO_3$ substrate in different orientations [(001), (110), and (111)]. We have optimized the etching time for both kinds of etching processes. A high-quality step–terrace structure without etch pits is obtained for 2% BHF and 100% ACID solution having a pH value of $\sim$ 3.30. For BHF etching, the optimum etching time depends on the substrate orientation [30 s for STO (001), 40 s for STO (110), and 60 s for STO (111)]. On the other hand, for ACID etching, the optimum etching time is more or less constant for all the orientations. This study might be extended to similar oxides substrates, especially on the exciting $KTaO_3$.

Keywords: Heterostructures; Transition metal oxides; Etching; $SrTiO_3$

1. Introduction

Transition metal oxides (TMOs) offer a rich unexplored field of fundamental research, along with their possible applications in the industry as well. The TMOs have a simple cubic structure ABO_3, where A is an alkaline earth atom, and B is a transition metal. The ABO_3 structure consists of alternating planes of AO and BO_2 in (001) directions. The simple cubic structure offers the opportunity to make heterostructure and super-lattices rather easily. $SrTiO_3$ (STO) is a noble transition metal oxide having a large dielectric constant [1], quantum paraelectricity [2], and simple cubic structure with lattice parameter 3.905°A, widely used substrate for making heterostructures and thin film fabrication [3, 4]. The STO substrate got more attention in the scientific community after the realization of conducting interface of $LaAlO_3$ (LAO) and STO [5]. The conductivity depends on the termination layer of the substrate [STO (001) in this case] surface. In the case of the STO (001), the charge-neutral atomic layers of SrO and TiO_2 are stacked alternatively, but in the case of LAO, the atomic layers LaO and AlO_2 are charged $+1$ and -1 alternatively. When the film of LAO is grown on an STO substrate, there are two possible interface formations (a) LaO/TiO_2 and (b) AlO_2/SrO. The LaO/TiO_2 interface is conducting, whereas the AlO_2/SrO interface is insulating in nature. This suggests the importance of the termination of the substrate surface. To make the interface conducting, STO needs to be TiO_2 terminated. These oxide heterostructures got more attention when exotic properties including Shubnikov–de Haas Oscillations [4], superconductivity [6], the coexistence of superconductivity and magnetism [7], photo-induced conductivity [8, 9], and many more are realized in this conducting interface. Along with STO (001), STO (110), and STO (111) orientation-based interfaces have also shown bizarre properties like high mobility and superconductivity, and many more [10]. Unlike STO (001), STO (110), and STO (111) have high surface energy which makes it difficult to achieve a single terminated surface. Hence, these require different surface treatments at different conditions [11]. Reports are available for surface termination for all orientations for STO [11, 12]. Here, we report how various etchants and their concentration, as well as the duration of the etching process, affecting the surface morphology.

There are various methods to obtain a single terminated STO substrate. These are mainly divided into two major categories (1) deionized (DI) water etching and (2) chemical etching (also known as wet etching). Chemical etching is done using different etching agents, some of them are

*Corresponding author, E-mail: suvankar.chakraverty@inst.ac.in

© 2023 IACS

HCL + NH_4Cl, HCl + HNO_3, Buffered NH_4F-HF (BHF), and so on. After etching, the surface morphology is confirmed by various characterization techniques like atomic force microscopy (AFM), ion scattering, and photoelectron scattering. In this paper, we have used AFM to characterize the surface morphology of the STO (001), (110), and (111) substrates and realized single terminated step and terrace formation at the surface of STO (001), (110), and (111) single crystals by thermal treatment followed by chemical etching method. In the chemical etching method, we have used the BHF etching and ACID etching (HCL + HNO_3 in 3:1). The concentration or pH value of the etchant and etching timing is the two main parameters that affect the termination and morphology of the substrate surface.

Here, we have varied both parameters to optimize the step–terrace structure formation (or removal of SrO particles) on the surface of STO single crystal.

2. Results and discussion

The crystal structure and morphology of the substrate depending on the polishing method used. Generally, there is corrugation of up to 2-unit cells present in the non-terminated substrates. Mechanical polishing led to defects on an atomic level. The defect-induced surface with impurities like carbon and organic compounds affect the interface and hence the interfacial properties. To achieve

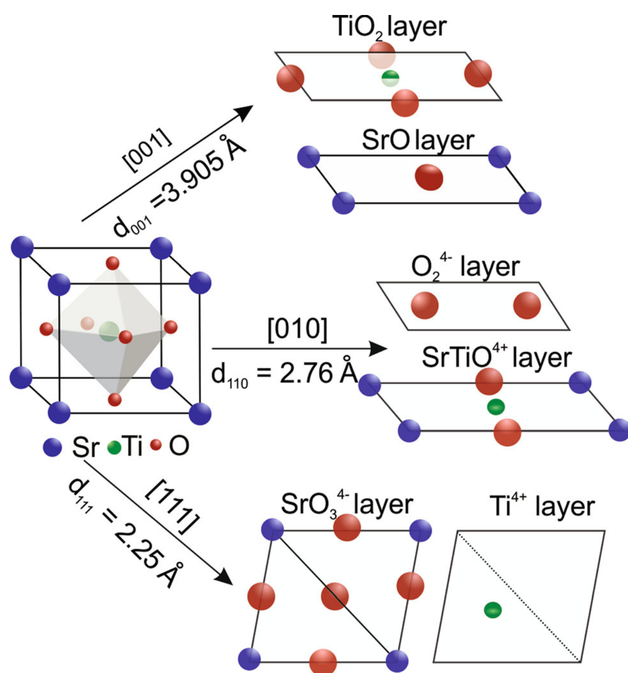

Fig. 1 (Left panel) Crystal structure of STO (001) unit cell, where Sr is at the corners of the unit cell and Ti lies at the center of the cube. Each Titanium atom is surrounded by 6 oxygen atoms. The right panel is representing the stacking of the atomic layers of STO in a different orientation. The distance between two atomic layers is 3.905°A, 2.76°A, and 2.25°A in (001), (110), and (111) orientations, respectively

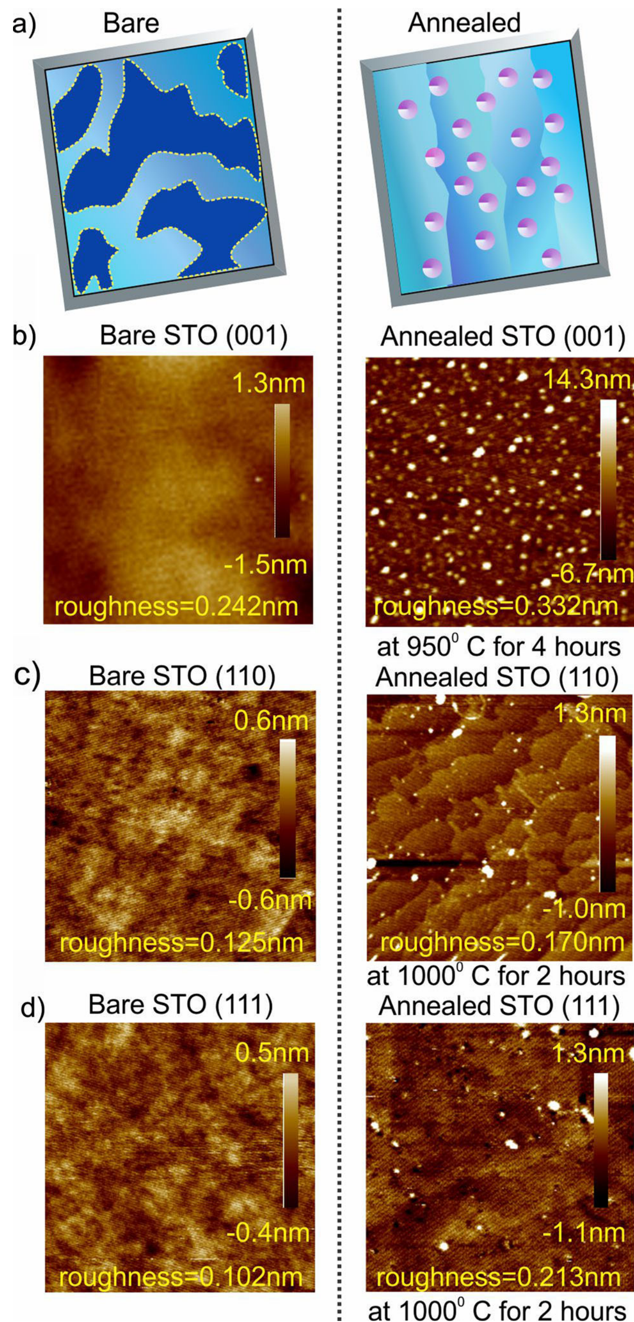

Fig. 2 (**a**) (Left panel) Schematic of the as-received mixed terminated STO substrate, (right panel) the schematic of the annealed substrate. (**b**) (Left panel) AFM image of as-received STO (001) substrate having roughness 0.242 nm, (right panel) AFM image of annealed STO (001) showing agglomerated SrO particles. (**c**) (Left panel) The AFM image of as-received STO (110) substrate having a roughness of 0.125 nm, (right panel) AFM image of annealed STO (110). (**d**) (Left panel) The AFM image of as-received STO (111) substrate having a roughness of 0.102 nm, (right panel) AFM image of annealed STO (111)

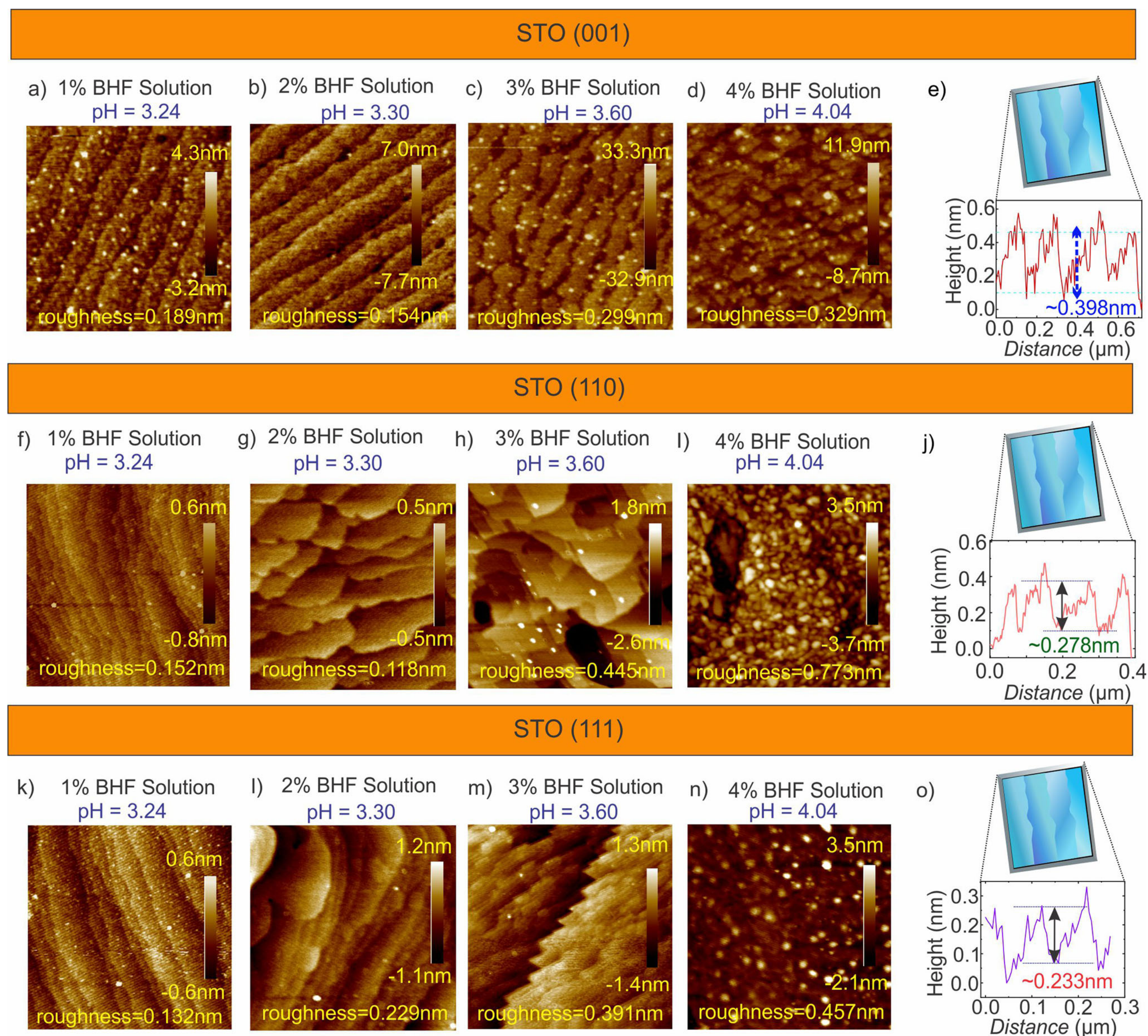

Fig. 3 (**a**, **b**) STO (001) surface after etching with 1% and 2% BHF solution, respectively. (**e**) The upper panel shows the schematic of the step–terrace structure on the STO surface, and the lower panel represents the height profile of the 2% BHF etched STO (001) surface. (**c**, **d**) The STO (001) surface after etching with 3% and 4% BHF solution, respectively. Similarly, (**f–i**) The STO (110) surface after etching with 1%, 2%, 3%, and 4%, respectively, (**j**) upper panel represented the schematic of the step–terrace structure on the STO surface, the lower panel presents the height profile of STO (110). (**k–n**) The STO (111) surface after etching with 1%, 2%, 3%, and 4%, respectively, (**o**) upper panel represented the schematic of the step–terrace structure on the STO surface, the lower panel presents the height profile of STO (111)

desired surface morphology, we took one side mechanically polished mixed terminated commercially available 10×10 mm STO single crystal. Firstly, we cleaned the as-received STO substrates with acetone and ethanol each, respectively, for 10 min in an ultrasonic bath, to remove the hard metal and unwanted particles present on the surface.

The crystal structure of simple cubic STO is shown in Fig. 1 (left panel). The right panel of Fig. 1 is representing the atomic layers of STO in different orientations. The interplanar distance for STO (001), (110), and (111) is 3.905°A, 2.76°A, and 2.25°A, respectively [12].

To study the surface morphology, we have taken the surface image of as-received STO single crystals using tapping mode AFM. The surface contained mixed termination of atomic layers, nonpolar SrO and TiO_2 in case of STO (001), $SrTiO^{4+}$ and O_2^{4-} polar layers for STO (110), and STO (111) is stacked as SrO_3^{4-} and Ti^{4+} polar atomic layers [12]. The schematic of the as-received substrate is shown in Fig. 2(a) left panel, the dark, and light blue colors

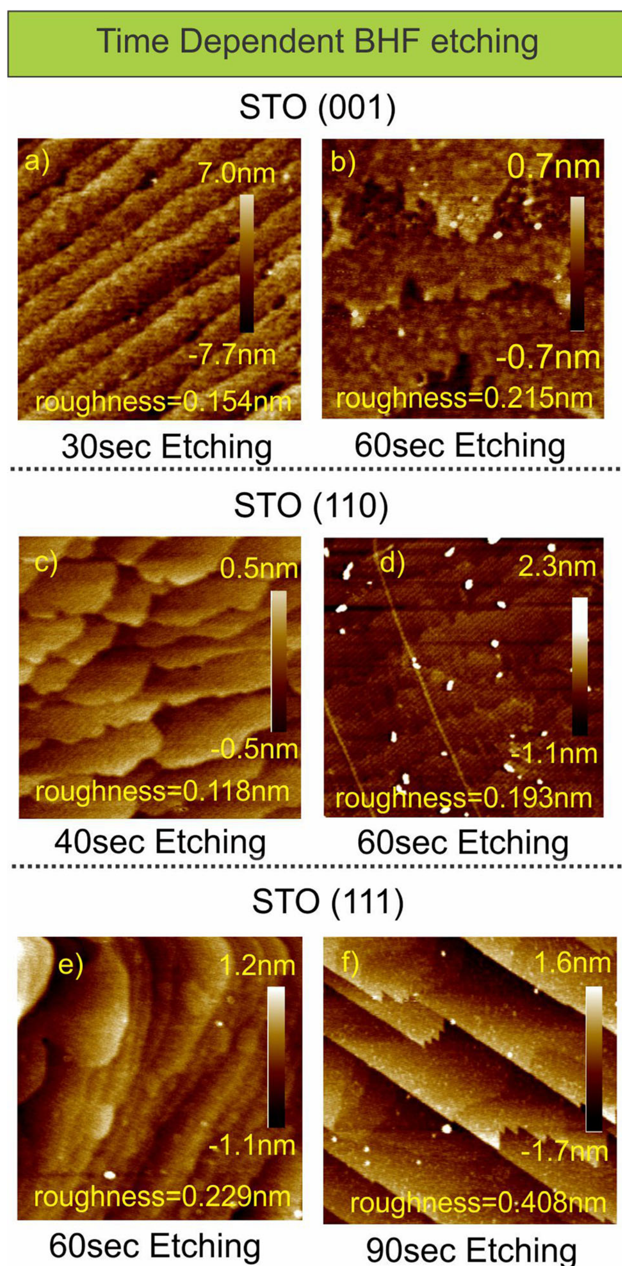

Fig. 4 (Upper panel) (**a**, **b**) Time-dependent etching of STO (001) surface for 30 s and 60 s, respectively. (Middle panel) (**c**, **d**) The time-dependent etching of STO (110) surface for 40 s and 60 s, respectively. (Lower panel) (**e**, **f**) The time-dependent etching of STO (111) surface for 60 s and 90 s, respectively

are defining two different atomic layers. Figure 2(b), (c), (d) (left panel) is representing the AFM of the as-received STO (001), (110), and (111). The roughness of the sample suggests the presence of small corrugation at the surface due to the presence of mixed atomic layers. This roughness or corrugation is not suitable for thin film deposition, to improve the surface quality, high-temperature annealing in an oxygen environment is done followed by chemical etching. We have annealed the substrates at different temperatures, the optimized annealing temperatures are 950° C for 4 h, 900° C for 2 h, and 1000° C for 2 h for STO (001), (110), and (111), respectively. The substrates with different orientations have different surface energy, thus, requiring different annealing temperatures. The heating at a high temperature increases the kinetic energy of the atoms, hence the agglomeration of the particle takes place at the surface, as shown in Fig. 2(a) right panel. The right panel (Fig. 2(a)) shows the schematic of the surface of annealed STO substrate. The right panel of Fig. 2(b), (c), (d) is representing the AFM image of annealed STO (001), (110), and (111) substrate in which the particles are agglomerated on the STO surface.

In 1994, Kawasaki et al. [13] demonstrated a chemical (using BHF) route of etching to achieve a single terminated substrate surface. The best step termination achieved in their case was at pH $\sim$ 4.5, but the surface contains etch pits. They assumed the polishing and crystal defects are responsible for the formation of the pits. The work is followed by Koster et al. and Hallsteinsen et al. [14, 15] where they obtained the single terminated STO (001), and (111) substrate, respectively, by firstly formation of Sr-hydroxide complex followed by BHF treatment. The method helps to remove etch pits formed in the former case. The pit formation deteriorates the thin film quality and also degrades the properties. In 2012, Wang et al. [16] reported the single termination of STO (110) using molecular beam epitaxy with minimum deviation from cation stoichiometry of $< 0.5\%$.

In this work, we have studied the etching of the STO surface using BHF and ACID by varying the pH value and time of etching. To make a BHF solution, 4 g of NH_4HF_2 (powder, Fisher Scientific, NH_4HF_2 = 57.04) was taken into a glass beaker and mixed with 6 ml of deionized (DI) water to make a 40% solution. A clear solution was obtained by heating the mixed solution at 60° C using a magnetic stirrer for 30 min to 1 h. The above solution was transferred to the Teflon beaker in a warm state only otherwise, the solution start forming crystals of NH_4HF_2. The temperature of the solution should not fall below 40° C. To obtain BHF solution 1 ml of HF (about 40% HF, Fisher Scientific, HF = 20.01) was added to the 40% NH_4HF_2 solution. The pH of obtained BHF solution can be varied by diluting it with DI water. We added 1 ml of BHF solution to 99 ml of DI water to obtain 1% BHF solution and the pH value was measured. Using the same technique, we prepared different concentrations of BHF solutions varying from 2%, 3%, 4%, and so on, thus, having different pH values.

The pH value and the etching time are the main parameters that control the surface morphology and stoichiometry of the substrate. The substrate is rinsed with DI water after etching and then dried using nitrogen gas.

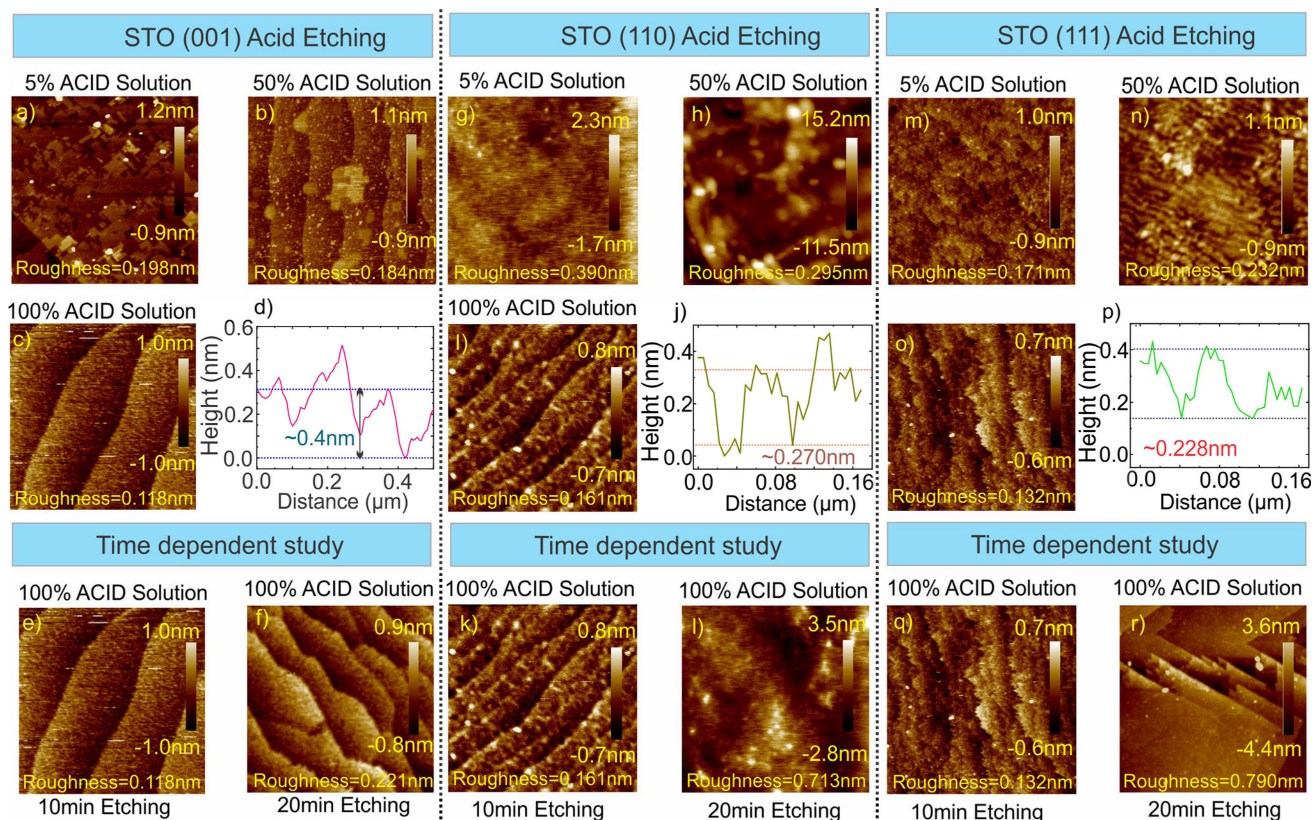

Fig. 5 (Left panel) (**a–c**) STO (001) surface after etching with 5% and 50%, and 100% ACID solution, respectively. (**d**) Represents the height profile of the 100% ACID etched STO (001) surface. (**e**, **f**) The STO (001) surface after etching with 100% ACID solution with etching time 10 min and 20 min, respectively. (Middle panel) (**g–i**) The STO (110) surface after etching with 5% and 50%, and 100% ACID solution, respectively. (**j**) Represents the height profile of the 100% ACID etched STO (110) surface. (**k**, **l**) The STO (110) surface after etching with 100% ACID solution with etching time 10 min and 20 min, respectively. (Right panel) (**m**, **o**) The STO (111) surface after etching with 5% and 50%, and 100% ACID solution, respectively. (**p**) Represents the height profile of the 100% ACID etched STO (001) surface. (**q**, **r**) The STO (001) surface after etching with 100% ACID solution with etching time 10 min and 20 min, respectively

Figure 3(a) is showing the AFM image of the STO substrate after being etched with 1% BHF solution. In our case, the best step–terrace structure is observed for a pH value of $\sim$3.30 (2% BHF solution) as shown in Fig. 3(b). The upper panel of Fig. 3(e) is the schematic figure for step–terrace-like structure formation on the STO surface after etching and the lower.

The panel of Fig. 3(e) represents the height profile of the 2% etched substrate. The height profile shows that the steps formed have an average height of 0.398 nm which is very close to the lattice parameter of the STO (001) (0.3905 Å) single crystal. If we increase the pH of the solution, the formation of the pit starts at higher pH values as seen in Fig. 3(c), (d). When the pH of the BHF solution is increased, there is an increase in the roughness of the surface. The pit formation starts on the surface when etched with a high concentration (3% and 4%) of BHF solution deteriorating the substrate as shown in Fig. 3(d).

A similar result is shown for STO (110) (middle panel of Fig. 3 (Fig. 3(f–j))), and STO (111) (Lower panel of Fig. 3 (Fig. 3(k–o))). As BHF is a highly reactive chemical, a high concentration of the BHF in the solution damages the surface of the STO single crystal, and hence the pits are formed. To optimize the etching time for BHF treatment, we performed etching at a different time at the same pH value. For the 2% solution ($\sim$3.30), we had done etchings at different times for all orientations of the STO substrate. In Fig. 4, we have shown the selective time AFM images for STO (001), (110), and (111), respectively. The best step-like structure was obtained for 30 s, 40 s, and 60 s etching times for STO (001), (110), and (111), respectively, as shown in Fig. 4(a), (c), (e). The different etching time for different orientation indicates the different surface relaxation energy of crystal in different crystallographic axis. The surface relaxation energy (−1.66 eV) for Ti-terminated STO (111) is five times larger than the SrO_3 terminated surface (−0.35 eV), similarly, for STO (110) the surface relaxation energy for Ti-terminated surface is −5.78 eV which is larger than the Sr-terminated layer (−0.86) [17, 18]. From the AFM images (Fig. 4(b), (d),

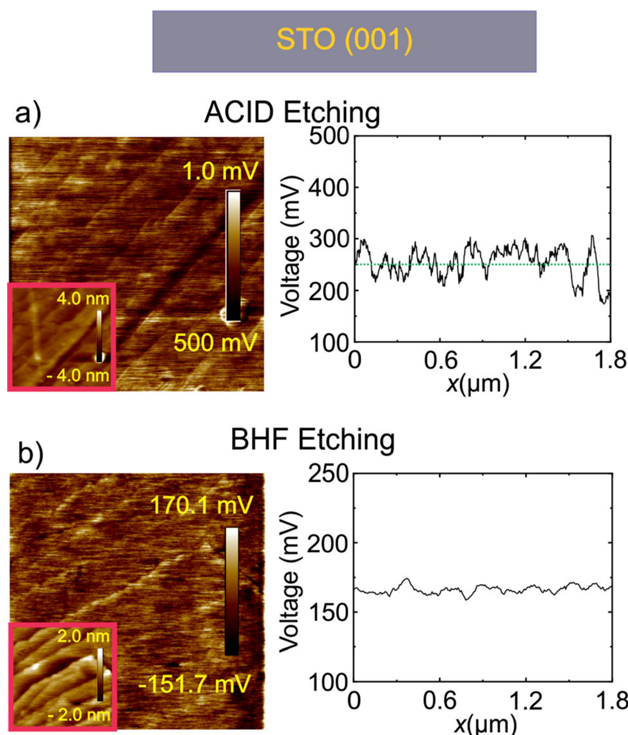

Fig. 6 LFM image and LFM line profile of STO (001) after ACID (**a**), and BHF etching (**b**). The inset is showing the height profile of the corresponding

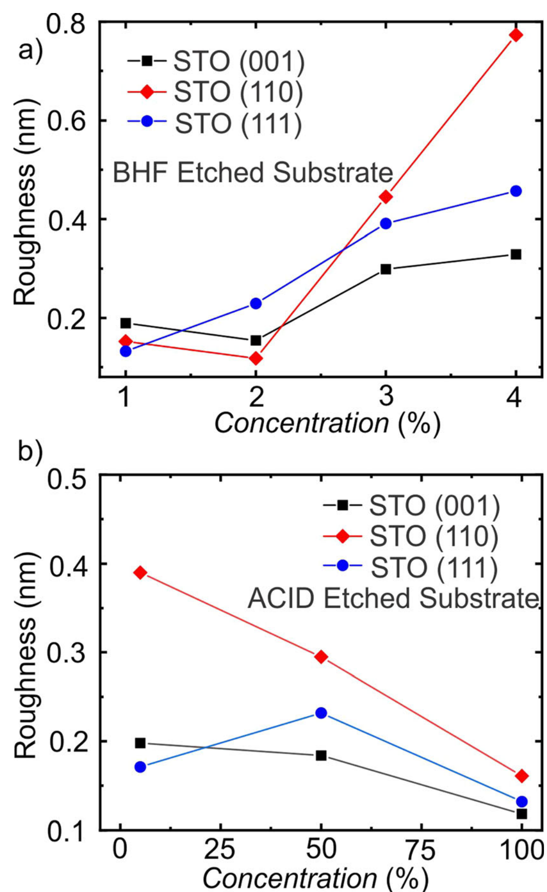

Fig. 7 Roughness of substrate surface as a function of concentration for BHF etching (**a**), and ACID etching (**b**)

(f)), we observed that as we increase the etching time the reaction time increases with the substrate surface. For higher etching time the steps started deforming (stacking of multiple steps) and there was a commencement of pit formation observed at the substrate surface. Figure 4(f) represents the stacking of steps for STO (111) for 90 s of etching time with a roughness of $\sim$0.408 nm. The best etching time and pH value for step–terrace-like structure formation on STO (001), (110), and (111) substrate surface by BHF are 30 s, 40 s, and 60 s with 3.30 pH values, respectively.

Similarly, for ACID etching we have prepared a solution by adding HCL (fuming 37%, Merck) to HNO_3 (69%, Merck) in a 3:1 ratio. The solution is diluted using DI water. We have used the following three concentrations to etch the STO (001) substrate, 5%, 50%, and 100%. For 5% ACID solution, 5 ml of ACID is mixed with 95 ml of DI water, and similarly for 50% and 100% solution. From Fig. 5(a), we observed that for 5% ACID solution, the SrO particles remained on the surface of the STO (001) substrate.

Hence, we have increased the concentration of the solution from 5 to 50%, for the 50% solution there are still some particles that remains on the surface of the STO (001) substrate, as shown in Fig. 5(b). The best step–terrace-like structure is obtained for 100% ACID solution with a 10 min etching time (Fig. 5(c)). Figure 5(d) is representing the height profile of the step-terminated STO (001) surface shown in Fig. 5(c). From the height profile, we can observe that an average height of $\sim$0.4nm step–terrace-like structure is obtained for STO (001) substrate. The height of the step is close to the lattice constant of the STO crystal. Similar results are obtained for both STO (110) and (111) (Fig. 5(g–i) for STO (110) and Fig. 5(m–r) for STO (111)). We have also studied the effect of etching time on the morphology of the substrate surface. In the time-dependent study (Fig. 5(e–f), (k–l), (q–r)), we have observed that as we increase the etching time, the steps start deteriorating, and also the increase in roughness is observed, hence no longer smooth surface. From this, we conclude that for our sample both ACID and BHF etching are most efficient at 100% and 2% concentration with an etching time of 10 min and 30 s, respectively. We have also done Lateral Force microscopy (LFM) measurements to confirm the surface termination of STO substrates. Figure 6(a), (b) is showing the LFM images and LFM line profile of the STO (001) substrate after ACID and BHF etching. The uniform frictional response in LFM topography implies single

termination of STO substrates. The inset of Fig. 6(a), (b) is showing the height image of the corresponding LFM images. Figure 7 is the summary showing all summarized results obtained for both BHF and ACID treatment.

3. Conclusions

In conclusion, we have successfully optimized the concentration of BHF solution and etching time to realize a step–terrace-like structure for the STO substrate. The best pH for etching is 3.30 for a 2% BHF solution. For higher pH value solutions, pits are observed on the surface. The step–terrace formation also depends on etching timing, which is 30 s, 40 s, and 60 s for STO (001), (110), and (111) in BHF solution etching, respectively. In addition, the ACID etching method is also explored. For ACID etching, the best concentration is 100% with a 10 min etching time. On comparing the results of both etchant treatments, we can conclude that BHF etching is a more controlled and better surface treatment method than ACID treatment.

In BHF etching the pH controlling is much easier than ACID treatment. Because of uncontrolled pH value, the acid treatment is not reproducible. These optimizations are not restricted to STO only and can be extended to other perovskite oxide. It will be especially interesting to perform a similar study on the newly emerging material in the oxide family "$KTaO_3$" [19].

Acknowledgements This project was supported by Grant No. 58/14/17/2019-BRNS/37024 (BRNS).

Declarations

Conflict of interest The authors declare no conflict of interest.

References

[1] H Fujishita, S Kitazawa, M Saito and R Ishisaka *J. Phys. Soc. Jpn.* **85** 074703 (2016)

[2] D Shin, S Latini, C Schafer, S A Sato, U De Giovannini, H Hubener and A Rubio *Phys. Rev.* **B104** L060103 (2021)

[3] N Wadehra, R Tomar, R M Verma, R K Gopal, Y Singh, S Duttagupta and S chakraverty *Nat. Commun.* **11** 874 (2020)

[4] N Kumar, N Wadehra, R Tomar, Shama, S Kumar, Y Singh, S Duttagupta and S chakraverty *Adv. Quantum Technol.* **4** 2000081 (2021)

[5] A Ohtomo and H Y Hwang *Nature* **427** 423 (2004)

[6] S Gariglio, N Reyren, A D Caviglia and J M Triscone *J. Phys. Condens. Matter* **21** 164213 (2009)

[7] D A Dikin, M Mehta, C W Bark, C M Folkman, C B Eom and V Chandrasekhar *Phys. Rev. Lett.* **107** 056802 (2011)

[8] S Goyal, N Wadehra and S Chakraverty *Adv. Mater. Interfaces* **7** 2000676 (2020)

[9] S Goyal, A Singh, R Tomar, R Kaur, C Bera and S Chakraverty *Solid State Commun.* **316** 113930 (2020)

[10] G Herranz, F Sánchez, N Dix, M Scigaj and J Fontcuberta *Sci. Rep.* **2** 758 (2012)

[11] S Woo, H Jeong, S A Lee, H Seo, M Lacotte, A David, H Y Kim, W Prellier, Y Kim and W S Choi *Sci. Rep.* **5** 8822 (2015)

[12] A Biswas, P B Rossen, C H Yang, W Siemons, M H Jung, I K Yang, R Ramesh and Y H Jeong *Appl. Phys. Lett.* **98** 051904 (2011)

[13] M Kawasaki, K Takahashi, T Maeda, R Tsuchiya, M Shinohara, O Ishiyama, T Yonezawa, M Yoshimoto and H Koinuma *Science* **266** 1540 (1994)

[14] G Koster, B L Kropman, G J H M Rijnders, D H A Blank and H Rogalla *App. Phys. Lett.* **73** 2920 (1998)

[15] I Hallsteinsen, M Nord, T Bolstad, P Vullum, J E Boschker, P Longo, R Takahashi, R Homestand, M Lippmaa and T Tybell *Cryst. Growth Des.* **16** 2357 (2016)

[16] Z Wang, J Feng, Y Yang, Y Yao, L Gu, F Yang, Q Guo and J Guo *Appl. Phys. Lett.* **100** 051602 (2012)

[17] R I Eglitis *NATO Science for Peace and Security Series B: Physics and Biophysics*, p. 125 (2012)

[18] E Heifets, W A Goddard, E A Kotomin, R I Eglitis and G Borstel *Phys. Rev. B* **69** 035408 (2004)

[19] A Gupta, H Silotia, A Kumari, M Dumen, S Goyal, R Tomar, N P WadehraAyyub and S Chakraverty *Adv. Mater.* **34** 2106481 (2022)

Publisher's Note Springer Nature remains neutral with regard to jurisdictional claims in published maps and institutional affiliations.

Springer Nature or its licensor (e.g. a society or other partner) holds exclusive rights to this article under a publishing agreement with the author(s) or other rightsholder(s); author self-archiving of the accepted manuscript version of this article is solely governed by the terms of such publishing agreement and applicable law.